БОТАНИЧЕСКИЙ ЖУРНАЛ, 2020, том 105, № 1, с. 15–31

СООБЩЕНИЯ

COMPARATIVE STUDY OF OVULE STRUCTURE AND DEVELOPMENT IN SOME SPECIES OF *IRIS* SUBGENUS *LIMNIRIS* (IRIDACEAE)

© 2020 г. M. M. Dorofeeva[1,2,*], P. M. Zhurbenko[1,**]

[1] *Komarov Botanical Institute of RAS*
Prof. Popov St., 2, St. Petersburg, 197376, Russia
[2] *Saint Petersburg State Forest Technical University*
Institutsky Lane, 5, St. Petersburg, 194021, Russia
**e-mail: drofa88@mail.ru*
***e-mail: pj_28@mail.ru*

Received November 13, 2019; Revised December 02, 2019; Accepted December 03, 2019

We described important characters of the ovule and embryo sac, such as nucellar cap, funicular obturator, inner integumentary obturator and filiform apparatus into the sinergids for seven *Iris* species: *Iris chrysographes*, *I. ensata*, *I. pseudacorus*, *I. sanguinea*, *I. setosa*, *I. sibirica*, *I. typhifolia*. These characters have been shown to be variable and taxonomically useful in the genus.

Keywords: genus *Iris*, *Limniris*, systematics, ovule, embryo sac, obturator, nucellar cap
DOI: 10.31857/S0006813620010068

Iris is type and one of the largest genera of Iridaceae. According to various estimates it includes 200–340 species (Rodionenko, 1961; Alexeeva, 2008). The genus is widespread in the Northern Hemisphere, with the largest number of species in the region, occurring from the Mediterranean to Central Asia.

The number of described species continues to increase. Thus, among the new species described in *Iris* over the past decades there are *I. kamelinii* Alexeeva (Alexeeva, 2006), *I. nezahatiae* Güner ex Duman (Güner, 2007), *I. hellenica* Mermygkas, Kit Tan ex Yannitsaros (Mermygkas, 2010), *I. lokiae* Alexeeva (Alexeeva, 2013), *I. schmakovii* Alexeeva (Alexeeva, 2018).

There is new data on *Iris* phylogeny obtained using molecular methods, however, there is still no generally accepted taxonomic treatment of *Iris*. Some of the reasons are the large size of the genus, its wide distribution, species polymorphism and hybridization processes that play significant roles in *Iris* evolution (Alexeeva, 2005; Mavrodiev, 2014).

According to the classification by Mathew (1989) largely based on works by Dykes (1913), Lawrence (1953) and Rodionenko (1961) the genus is divided into six subgenera and 12 sections. The most morphologically, ecologically and taxonomically diverse subgenus of *Iris* is *Limniris*, which is divided into two sections. Section *Limniris* is the larger of the two and includes 16 series.

Mathew's classification is based on various features, among which the most important are sepal beards and/or crests, seed coat structure, presence or absence of seed arils and type of geophytic organs. Unlike Mathew, who considers the genus broadly, several systematists prefer a narrower circumscription of *Iris*. For instance, Rodionenko (2007) considered *Limniris* a separate genus. Another classification was advanced by Mavrodiev (2014), that suggested splitting *Iris* into 23 genera.

A number of recent studies (Tillie et al., 2001; Wilson, 2004, 2006, 2009, 2011; Mavrodiev, 2014) have shown that subgenus *Limniris* is polyphyletic, although a core *Limniris* clade is potentially monophyletic, comprising about 45 taxa from section *Limniris*. Based on molecular phylogenic studies, Wilson (2006) demonstrated that morphological features that were previously used in *Iris* classifications show extensive homoplasy. The homoplasy of the sepal crest was also established by Guo, Wilson (2013) using scanning electron microscopy, although most of crested irises form a monophyletic clade. Thus, the search for new synapomorphies for monophyletic groups is an important task.

Such synapomorphies can be provided by embryological data. Embryonic structures, as well as their development, are stable, conservative, and not significantly dependent on environmental changes, suggesting they may be especially important in systematic studies (Kamelina, 1980). Data on the morphogenesis of embryonic structures, along with data on paleobot-

any and comparative morphology, are considered important for phylogenetics (Poddubnaya-Arnoldi, 1930, 1958, 1976; Maheshwari, 1954; Kordyum, 1971; Kamelina, 1980).

The development of embryonic structures allows one to highlight a number of diagnostic features that may be important to systematics, such as: the type of tapetum and its patterns of organization, microspore tetrad formation, exine sculpture of pollen grains, the location and movement of generative cells, the number and shape of nuclei in pollen grains, the number and location of pollen grain pores and grooves, the number of ovule integuments, the form of micropyle, the presence of obturators, the shape and the size of nucellus, the presence of a hypostase the location of integuments, the nature of archesporial cell, the presence of parietal layers, the location of megaspores, the position of the viable megaspore, the type and shape of embryo sac, the number of nuclei, degeneration of synergids and antipodals, the increase of antipodal number, pollen tube growth in the ovule, the type of sexual nuclei fusion, endosperm ploidy and division, the presence of haustoria, the form and structure of embryo and its differentiation, the presence of chlorophyll in the embryo (Mageshvari, 1954; Kamelina, 1980; Poddubnaya-Arnoldi, 1982).

It should be noted that embryology of the genus *Iris* has not been well studied. Embryological studies have been published for only a few species: *Iris japonica* (Haeckel, 1930; Yasui, Sawada, 1940), *I. chamaeiris* (Haeckel, 1930), *I. pseudacorus* L. (Haeckel, 1930; Karagyozova, 1963; Rudall, 1984), *I. fulva* and *I. hexagona* var. *giganticaerulea* (Riley, 1942), *I. munzii* (Lenz, 1956), *I. tenax* (Smith, Clarkson, 1956; Rudall, 1984; Wilson, 2001), *I. pumila* (Sokolov, 1974, 1983), *I. sibirica* (Poddubnaya-Arnoldi, 1976), *I. kumaonensis* and *I. decora* (Pande, Singh, 1981), *I. germanica* and *I. pallida* (Sokolovskaya, Shpilevoj, 1990), *I. bloudowii* (Li et al., 2003), *I. mandshurica* Maxim (Zhang, 2011), and *I. sanguinea* (Fan et al., 2019). More than half of these species show abnormalities in the formation and structure of embryo sacs.

The purpose of this research is to study embryological characters mentioned above focusing on structures such as the nucellar cap, funiculus obturator and inner integument obturator to assess their usefulness in the systematics of the genus.

MATERIALS AND METHODS

Plant Materials and Growth Conditions

Materials of *Iris setosa* Pall. ex Link., *I. chrysographes* Dykes, *I. sanguinea* Donn ex Hornem., *I. typhifolia* Kitag., *I. ensata* Thunb. and *I. pseudacorus* L. were collected from specimens cultivated in the Iridarium of Botanical Garden of Komarov Botanical Institute of the Russian Academy of Sciences. *Iris sibirica* L. materials were collected at two sites in Perm territory, one near the Perm city on a rural locality Krasava and one near the Chaykovsky town in the National park "Krasnoe Plotbishche".

Specimen Preparation

Specimens were prepared from various developmental stages of whole buds and flowers. Ovules were harvested after performing crossing studies, and also from early development stages after natural flower pollination. For crossing studies, controlled cross-pollination and self-pollination within an individual were used.

The specimens were fixed immediately in Navashin's fixative (chromic acid 1%: formalin 16%: acetic acid, 10:4:1 v/v/v) or with use of Clarke's fixative (alcohol 96%: glacial acetic acid, 3:1 v/v), then dehydrated in ethanol series, infiltrated with xylene and embedded in paraffin wax by conventional methods (Pausheva, 1988). Embedded materials were sectioned at a thickness of 10–12 μm. Sections were stained with original Gallocyanin – chrome alum stain (Pearse, 1962; Barykina, 2004) and in triple stain following Kamelina et al. (1992) with use of Schiff's reagent, alcian blue and Ehrlich's Haematoxylin. After the staining, sections were mounted on slides in Bio Mount resin. Digital images were captured using an Olympus camera system and cell B software.

Sequence Alignment and Analysis

Sequence data of four plastid loci: *matK*, *trnL*, *trnL-F IGS*, *ycf1* was downloaded from GenBank/EMBL databases (Appendix S). Data was downloaded for the seven study species and an outgroup species, *I. ruthenica* Ker Gawl. Sequences were generated mostly by Wilson (2009), Wheeler and Wilson (2014), Dong et al. (2015), Fenneman (2016), Boltenkov (2018) and Mizuno et al. (2018) Sequences were manually edited and assembled using MEGA X (Kumar et al. 2018) prior to analysis. The alignment was performed using muscle (Robert, 2004). All indels were excluded from the analysis. The combined dataset of four loci had 2,269 bp.

The evolutionary history of the seven study species was inferred by using the Maximum Likelihood method and Tamura-Nei model (Tamura and Nei, 1993). Bootstrap support was determined with 1,500 replicates. Initial trees for the heuristic search were obtained automatically by applying Neighbor-Join and BioNJ algorithms to a matrix of pairwise distances estimated using the Maximum Composite Likelihood (MCL) approach, and then selecting the topology with superior log likelihood value. Obtained tree has a log likelihood –4039. Evolutionary analyses were conducted in MEGA X.

RESULTS

Ovule development. The structure and development of ovules in the studied species are similar. The species have syncarpous gynoecia and inferior ovaries.

In the ovary, ovules are arranged in two rows within each of three locules and have axile placentae (Fig. 1). Ovules are arranged in pairs (Figs. 1b, 1h, 1l) or in staggered formation (Figs. 1f, 1j, 1n). In *I. setosa*, isolated cases of ovules arranged in threes were observed (Fig. 1d). Ovules of studied species are anatropous and bitegmic, with a funiculus extended to the ovary (Fig. 2).

In *I. ensata* and *I. typhifolia* ovules curve to the anatropous position in early stages. By the beginning of megasporogenesis, the ovule is curved at 180°, the vascular bundle is differentiated, both integuments are developed and the micropyle is formed. In *I. sanguinea*, *I. setosa* and *I. sibirica* megasporogenesis begins when ovules are curved at 90–100°, the inner integument is developed, and the outer one is just initiatiated. The inner integument elongates due to the anticlinal divisions and extends beyond the nucellus, defining the zone that will become a micropyle.

During development of the ovule, due to uneven growth in the area of attachment of integuments, the ovule curves at 180°, so the micropyle turns towards the placenta, and the chalaza and micropyle are on the same axis at opposite poles of the ovule, which characterize the ovule as anatropous.

The outer integument is defined as a multilayered ring of cells (Fig. 2). In *I. setosa*, the outer integument has an irregular shape, consists of 5–6 layers, expands to 7–10 layers in the micropyle region and tapers to the edge. In *I. pseudacorus* the outer integument consists of 5–7 layers, in *I. sibirica* of 4–6 layers, and in *I. ensata* of 7–8 layers. In *I. sanguinea* the outer integument consists of 5 layers while in *I. chrysographes* and *I. typhifolia* the outer integument has 8–9 layers.

In *I. sanguinea*, *I. typhifolia* and *I. chrysographes*, from series *Sibiricae* the outer and inner integuments are of equal length (Figs. 2a, 2d, 2g). In *I. pseudacorus*, *I. ensata* and *I. sibirica*, from series *Laevigatae*, the outer integument is at least 48 ± 2 μm shorter than the inner (Figs. 2b, 2c, 2e). The outer integument of *I. setosa* from series *Tripetalae* is also at least 68 ± 16 μm longer than the inner (Fig. 2f).

The micropyle is formed by a two-layered inner integument. The length of the micropyle canal varies from 101 ± 9 μm (*I. setosa*) to 243 ± 9 μm (*I. sanguinea*).

The inner integument at the micropyle area expands to form up to 3 layers in *I. chrysographes* and *I. sibirica*, up to 3–5 layers in *I. sanguinea* and *I. pseudacorus*, up to 4 layers in *I. typhifolia*, up to 4–5 layers in *I. ensata* and up to 6 layers in *I. setosa*. The studied species form an operculum.

The inner integument cells lining the micropyle are radially elongated, glandular in appearance and form the integumentary obturator in ovule of *I. sibirica*. Such radially elongated cells in the micropyle area were observed in *I. tenax* (Wilson, 2001).

Layers of elongated cells with a dense cytoplasm differentiate in the funiculus, forming the vascular bundle. The vascular bundle differentiates towards the chalazal end of the ovule and consists of several cell layers.

The vascular bundle of *I. sibirica*, *I. sanguinea*, *I. typhifolia*, *I. ensata*, *I. setosa* and *I. pseudacorus* reaches the chalazal end of the ovule. The vascular bundle of *I. chrysographes* extends past the chalazal end of the ovule to the middle of the outer integument.

According to the structure and development of the nucellus, these ovules are crassinucellate and are characterized by differentiation in the nucellus of parietal tissue, a nucellar cap in some, and postament and podium cells (based on the classification of structures of nucellus basal area, Shamrov, 2008).

The layers of parietal tissue form during megasporogenesis (Fig. 3). The parietal cell divides anticlinally and periclinally resulting in 1–2 layers of cells in *I. ensata* and *I. chrysographes*, 2 layers in *I. setosa*, *I. typhifolia*, *I. sibirica* and up to 4 layers in *I. sanguinea*.

The layers of parietal tissue begin to compress at the uni-nuclear embryo sac stage. By the end of the first mitotic division, the parietal layers completely degenerate.

In the studied species of series *Laevigatae* as well as in *I. chrysographes*, the nucellar epidermis divides periclinally to form a nucellar cap. It has 2 layers in *I. ensata*, *I. sibirica*, *I. pseudacorus*, *I. chrysographes* and 2–3 in *I. setosa*.

In *I. sanguinea* and *I. typhifolia*, representing one clade, the nucellar epidermis does not divide periclinally and the embryo sac lies directly under the single-layered epidermis. The cells of the nucellar epidermis in the micropyle area become radially elongated and highly glandular in appearance, which we consider a nucellar obturator.

The postament and podium are differentiated in the basal area of nucellus (Shamrov, 2008). The form and size of postament and podium cells vary among species (Fig. 4). In the nucellus of *I. sanguinea* we observed layers of elongated cells with large nuclei that occur from the embryo sac to chalaza. Cells of the nucellus lateral area are of irregular shape and form the podium. In *I. setosa* the postament cells are square and podium cells are isodiametric and elongated in lateral area. In *I. typhifolia* the postament cells are elongated (the length is 3–4 times its width), with large nuclei, while podium cells are isodiametric. In *I. pseudacorus* the postament cells are elongated (the length is 2–3 times its width).

All studied species form a funicular obturator. The obturator cells are glandular in appearance, have thickened outer walls and dense cytoplasm (Fig. 2).

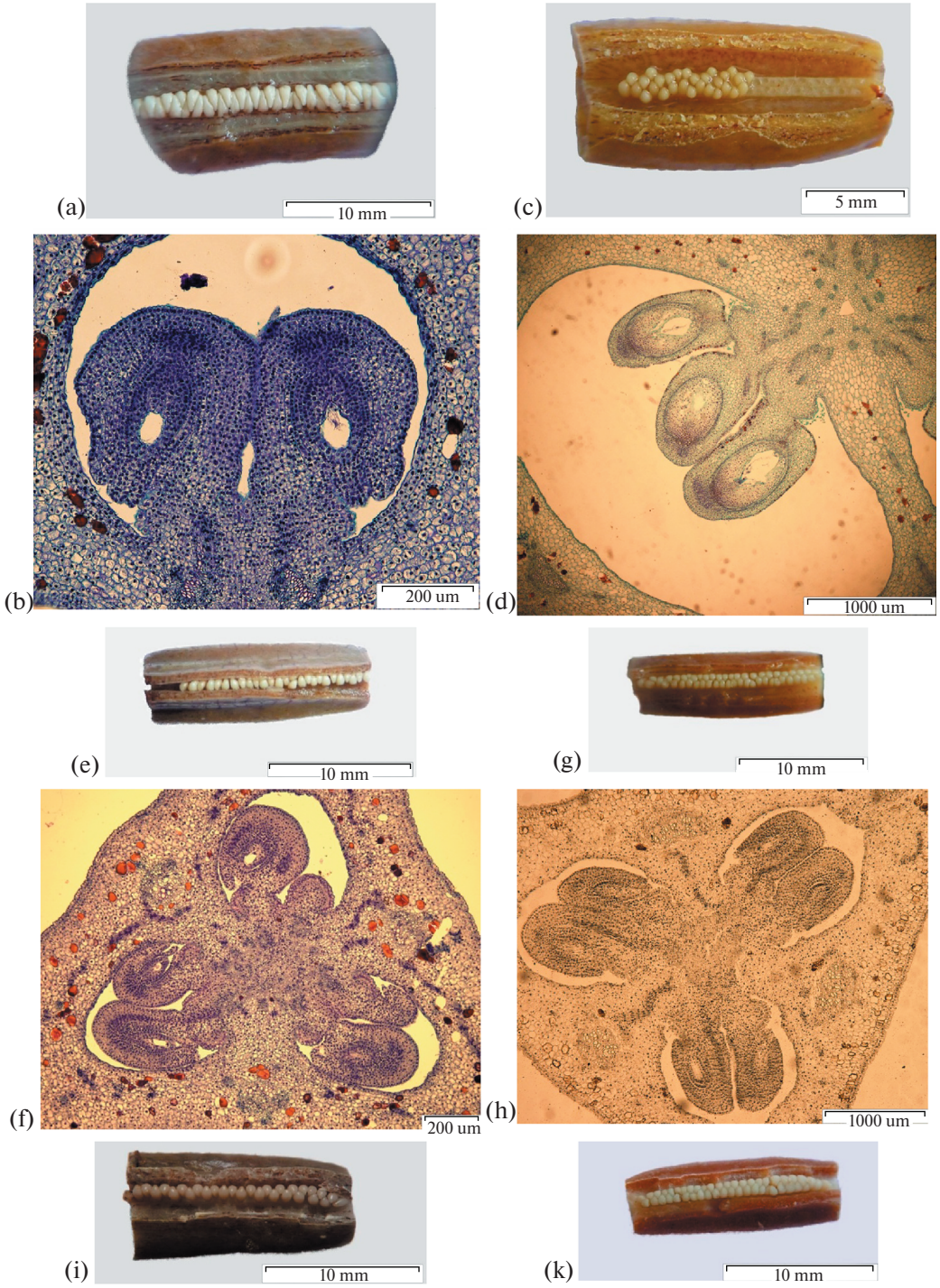

Fig. 1. The ovules in ovary locules. a – *I. ensata* (×10); b – *I. ensata* bud 70 mm (×100); c – *I. setosa* (×10); d – *I. setosa* ovary, 4-day after pollination (×40); e – *I. chrysographes* (×10); f – *I. chrysographes* bud 35 mm (×100); g – *I. sanguinea* (×10); h – *I. sanguinea* bud 40 mm (×40); i – *I. pseudacorus* (×10); j – *I. pseudacorus* ovary, 4-day after pollination (×100); k – *I. sibirica* (×10); l – *I. sibirica* (×40); m – *I. typhifolia* (×10); n – *I. typhifolia* bud 40 mm (×40).

an – antipodal; *cc* – central cell; *ch* – chalaza; *ec* – egg cell; *em* – embryo; *end* – endosperm; *es* – embryo sac; *fm* – functional megaspore; *fo* – funicular obturator; *ii* – inner integument; *io* – integumentary obturator; *m* – megasporocyte; *mi* – micropyle; *mn* – male nucleus; *nc* – nucellar cap; *no* – nucellar obturator; *oi* – outer integument; *op* – operculum; *pd* – podium; *pc* – parietal. cell; *pe* – primary endosperm nucleus; *ps* – postament; *pt* – parietal tissue; *ptu* – pollen tube; *sn* – secondary nucleus; *sc* – sperm cell; *sy* – synergid; *vb* – vascular bundle; *z* – zygote.

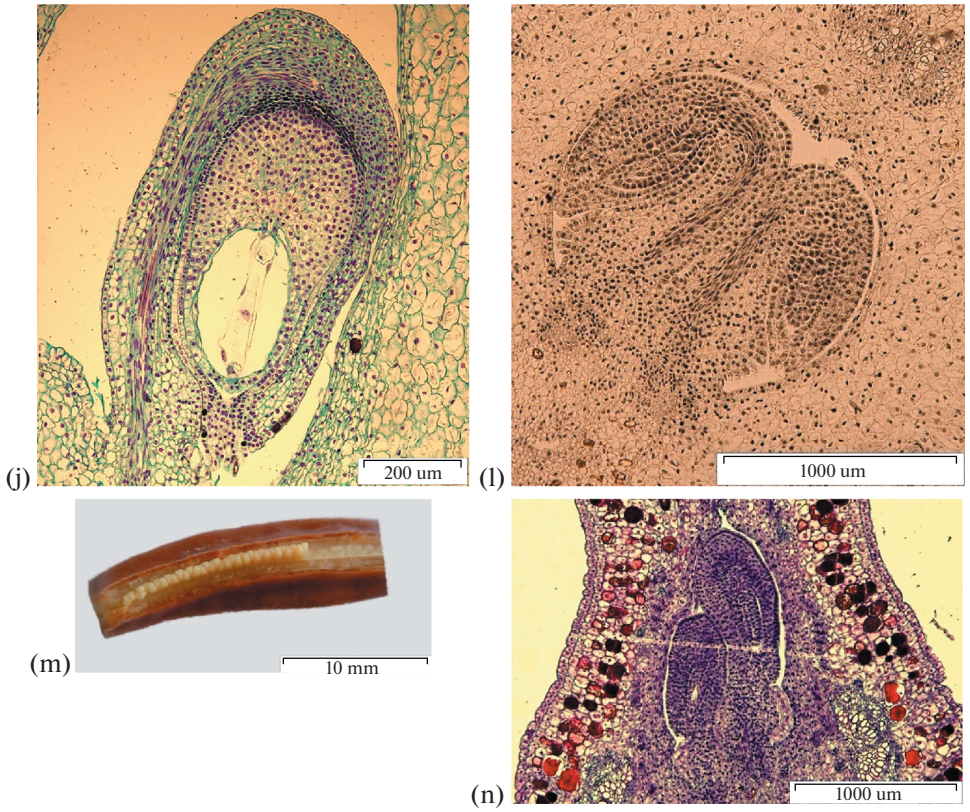

Fig. 1. (Contd.)

Megasporogenesis. During early stages of ovule development the archesporial cell differentiates, and after periclinal division forms the parietal cell and sporogenous cell, the later which then becomes the megasporocyte (Figs. 3a, 3b). The megasporocyte is characterized by a large nucleus, dense cytoplasm and can be easily defined from other nucellus cells. During the next two meiotic divisions the megasporocyte forms the linear tetrad of megaspores via cytokinesis.

In the megasporocyte of *I. setosa* the meiosis begins simultaneously with the anticlinal division of parietal cell (Fig. 3a). The dyad of cells forms after the first meiotic division of megasporocyte (Figs. 3c, 3g). In *I. setosa* the first partition originates high, determining two unequal cells. In *I. ensata* and *I. typhifolia*, the chalazal cell of the dyad is twice as large than the micropylar one.

The second meiotic division forms a linear tetrad of megaspores (Figs. 3d, 3f). In *I. setosa* the division by the micropylar pole sometimes occurs in a perpendicular orientation and four megaspores resemble a T-shaped structure (Fig. 3e). A triad of megaspores is formed in some ovules of *I. sanguinea* due to the lack of second meiotic division in the upper dyad cell (Fig. 3h).

In a single ovary of *I. ensata*, ovules can be observed at the stage of dyad as well as with completed tetrads of megaspores indicating completion of the second meiotic division.

In some tetrads of *I. setosa* the septum dividing the two megaspores at the micropylar end is curved 45° curved toward the chalazal megaspore.

In all studied species the chalazal megaspore is larger, possesses higher cytoplasm content and a larger nucleus than other sister cells of the tetrad. Micropylar megaspores degenerate and die (Figs. 4a, 4b, 4c).

Female gametogenesis. The chalazal megaspore is the functional spore (Figs. 4a, 4b, 4c). The first mitotic division leads to the formation of the two-nuclear coenocyte, with nuclei diverging to the poles of embryo sac (Figs. 4d, 4e, 4f).

Division of nuclei is accompanied by the formation of a central vacuole. The embryo sac enlarges toward the micropyle, resulting in compression of the parietal tissue and nucellar cells, which are directly adjacent to the embryo sac.

In some ovules of *I. setosa*, *I. chrysographes*, *I. sibirica* and *I. pseudacorus* a region of large, highly vacuolated cells develop adjacent to the embryo sac (Figs. 4d, 4h, 4i). Similar cells where described by Wilson (2001) who observed nuclei of enlarged cells adjacent to the embryo sac in *I. tenax*. These cells were obvious and could be seen pressed against the embryo sac.

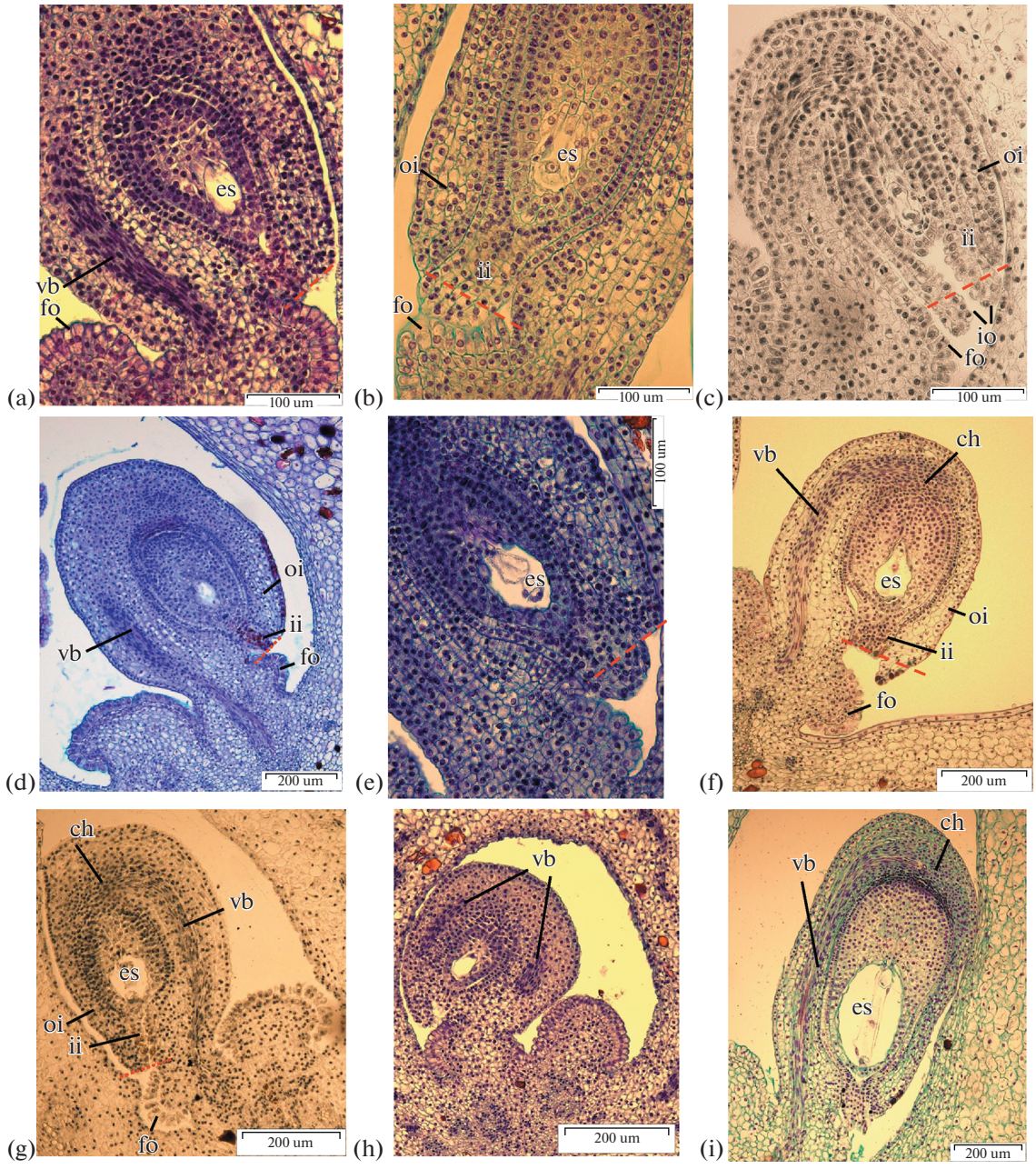

Fig. 2. Ovule development. a – *I. chrysographes*, ×400; b – *I. pseudacorus*, ×400; c –*I. sibirica*, ×400; d – *I. typhifolia*, ×100; e – *I. ensata*, ×400; f – *I. setosa*, ×400; g – *I. sanguinea*, ×400; h – *I. chrysographes*, ×400; i – *I. setosa*, ×100.

In *I. ensata* before a second mitotic division the embryo sac passes some through a rest period. The stage of the two-nucleate embryo sac in the ovules continues during the bud growth from 40 to 60 mm.

A second mitotic division results in the four-nucleate embryo sac (Figs. 4g, 4h). Nuclear divisions do not occur synchronously (Fig. 4g). By this time the embryo sac enlarges considerably, becoming more round and the cells adjacent to the embryo sac flatten. The nuclei remain at the poles and divide mitotically again, forming the eight-nucleate coenocyte (Fig. 4i).

With the end of mitotic divisions in the micropylar and chalasal poles of the embryo sac the cytoplasm localizes around the polar groups of nuclei, and cell formation begins (Figs. 4j, 4k). The period of the differentiation of embryo sac elements begins immediately after cell formation and is accompanied by intensive growth of the embryo sac.

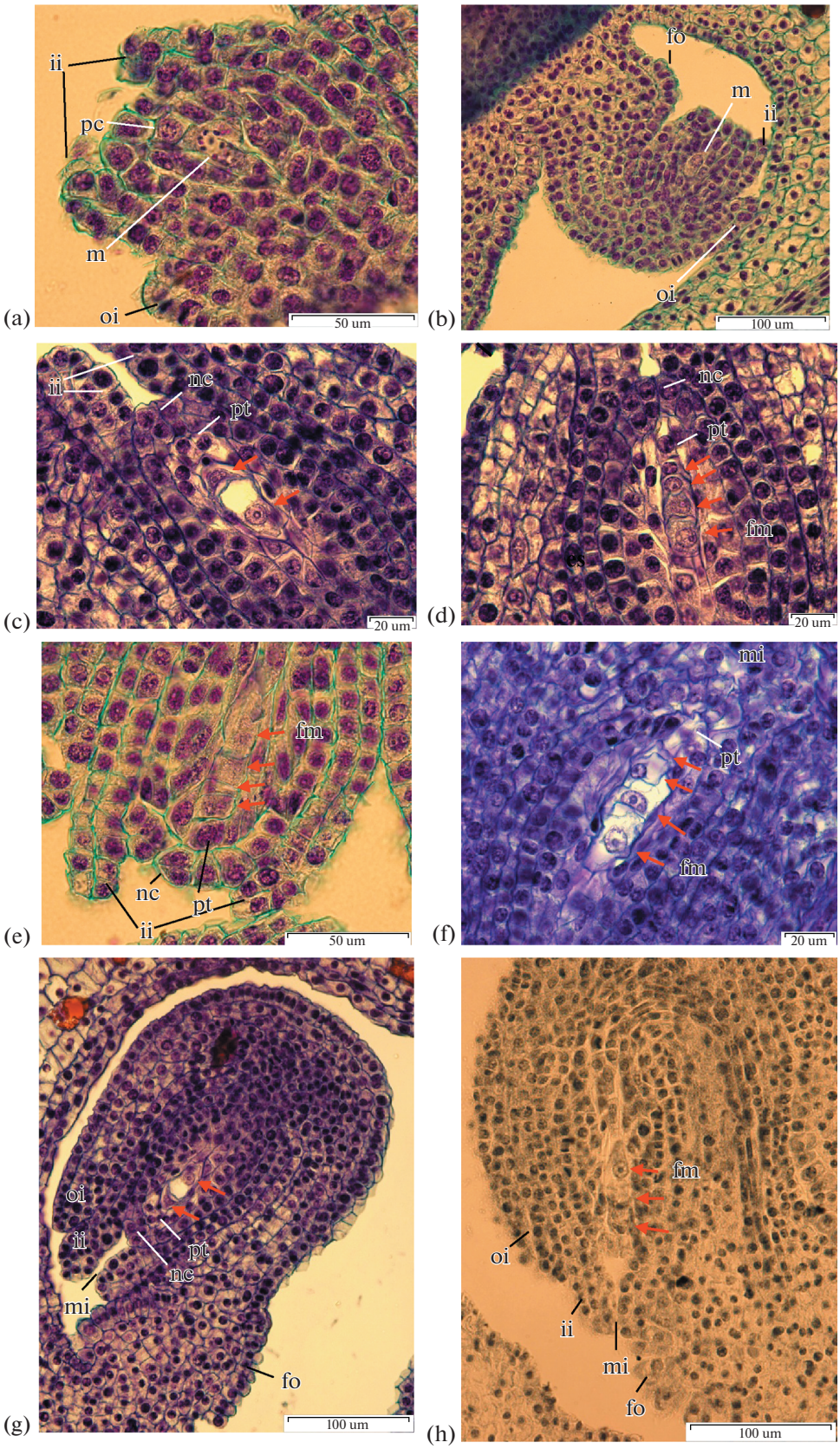

Fig. 3. Megasporogenesis. a – *I. setosa* bud 20 mm, ×1500; b – *I. setosa* bud 20 mm, ×400; c –*I. ensata* bud 35 mm, ×1500; d – *I. ensata* bud 35 mm, ×1500; e – *I. setosa* bud 20 mm, ×1500; f – *I. typhifolia* bud 35 mm, ×1500; g – *I. ensata* bud 35 mm, ×400; h – *I. sanguinea* bud 35 mm, ×400. c, g – at arrows dyad cell; d, e, f, h – at arrows megaspores.

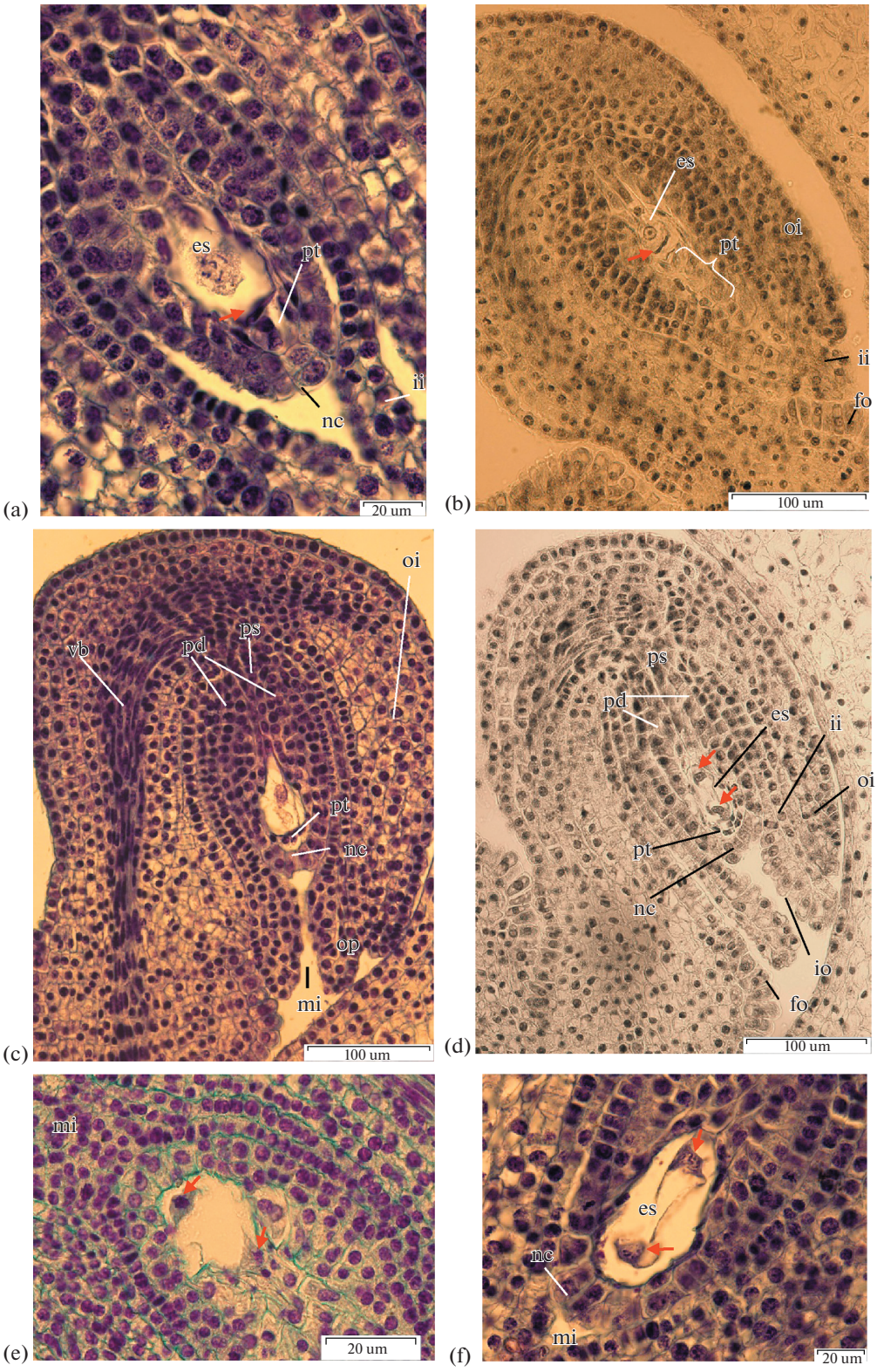

Fig. 4. Megagametogenesis. a – *I. chrysographes* bud 35 mm, one-nucleate embryo sac, at arrows megaspores degenerate, ×1500; b –*I. sanguinea* bud 40 mm, one-nucleate embryo sac, at arrows megaspores degenerate, ×400; c – *I. ensata* bud 40 mm, one-nucleate embryo sac, ×400; d – *I. sibirica* bud, two-nucleate stage of megagametogenesis, ×400; e – *I. pseudacorus* bud 40 mm, two-nucleate stage, at arrows nuclei, ×1500; f – *I. chrysographes* bud 35 mm, prophase in nuclei two-nucleate stage, ×1500; g – *I. typhifolia* bud, four-nucleate stage, ×1500; h – *I. pseudacorus* bud 40 mm, four-nucleate stage, ×1500; i–k – *I. chrysographes* bud 45 mm, ×1500, l – *I. sibirica*, three-celled egg apparatus, ×1500; m – *I. setosa*, two polar nuclei, ×1500; n – *I. setosa*, secondary nucleus within the central cell, ×1500; o – *I. setosa*, antipodals in chalazal pouch, ×1500.

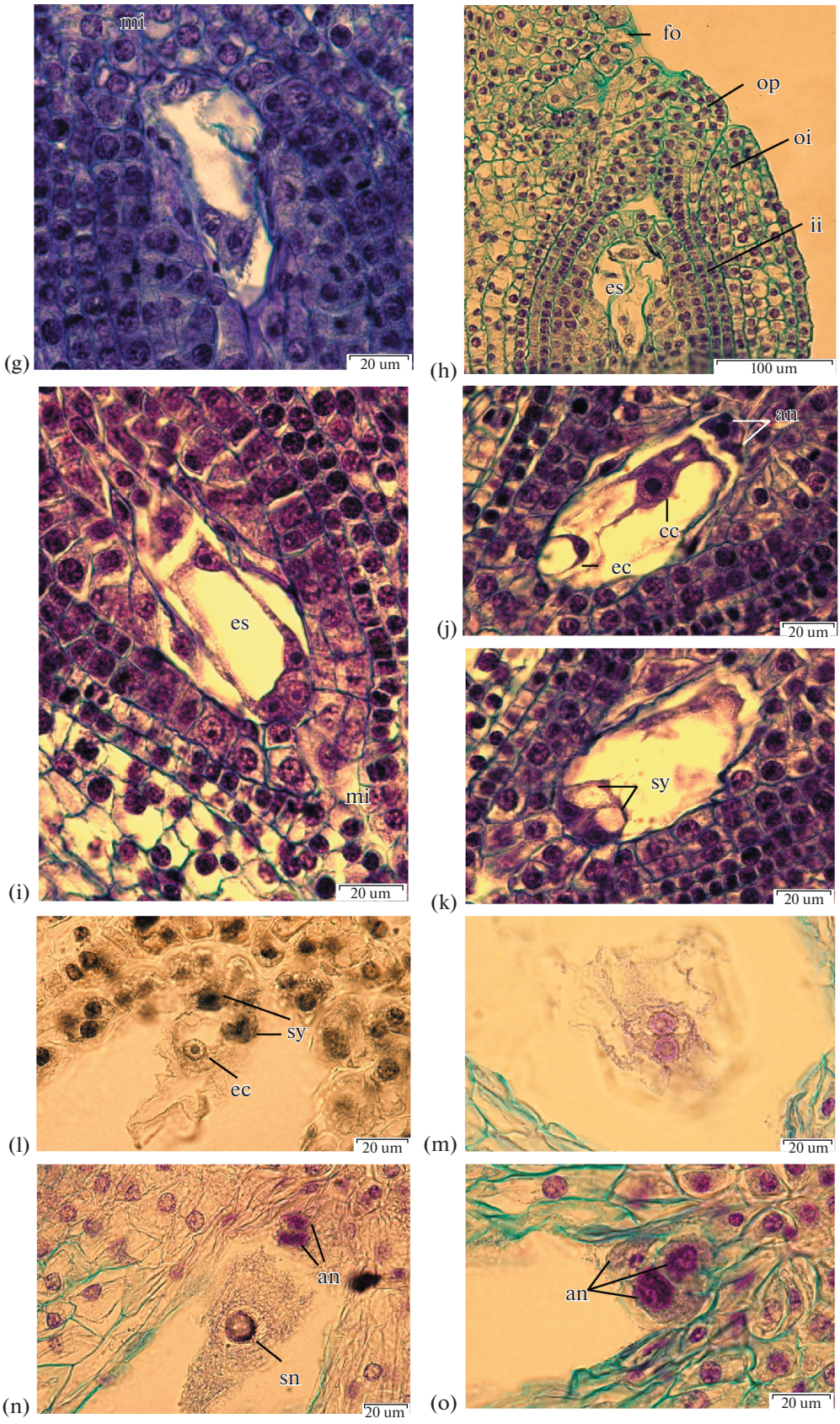
(g)
mi
20 um
(h)
fo
op
oi
ii
es
100 um
(i)
es
mi
20 um
(j)
an
cc
ec
20 um
(k)
sy
20 um
(l)
sy
ec
20 um
(m)
20 um
(n)
an
sn
20 um
(o)
an
20 um

Fig. 4. (Contd.)

Differentiation of the egg apparatus begins with cell vacuolization. The egg apparatus consists of the egg cell and two synergids (Fig. 4l). Synergid cells are located near each other with nuclei in the central area of their cells and vacuoles in the apical zones (Fig. 4k). In *I. sibirica* and *I. sanguinea* the filiform apparatus is clearly distinguishable at the base of the synergids (Fig. 4l). Also synergids are pressed tight to each other and the ovule is located behind them.

The egg cell is slightly larger than the synergids. The egg cell has another polarization: the nucleus is located in the apical zone of the cell, and the vacuole is in the basal zone (Fig. 4j). The place where ovule attaches to the wall of the embryo sac can be observed on the bilateral section of the ovule.

Soon after cell formation, the polar nuclei fuse, forming the secondary nucleus of the central cell (Figs. 4m, 4n). In *I. chrysographes* and *I. sanguinea*, fusion of the polar nuclei occurs at the flower bud stage. In *I. sanguinea* ovules at the stage of polar nuclei fusion as well as ovules, in which the secondary nucleus of the central cell has already formed can be observed in a single ovary.

In *I. setosa*, *I. pseudacorus* and *I. typhifolia* the polar nuclei fusion occurs after the flower opens. Lee W. Lenz (1956) reports that in many cases, at the time of the opening of *I. munzii* flower, the polar nuclei have not yet approached and the fusion may be delayed as much as 72 hours after pollination.

The central cell is pierced by thin strands of cytoplasm, with vacuoles between them. The secondary nucleus in the central cell is located in the center of embryo sac. In *I. sanguinea* and *I. typhifolia* the secondary nucleus of the central cell in some embryo sacs are located near the antipodals.

In the chalazal pole of embryo sac three antipodals differentiate (Figs. 4j, 4o). The increase of antipodal number to four is observed in *I. sibirica* and *I. setosa* (Figs. 6f, 4i). In *I. setosa* and *I. sanguinea*, the antipodals are elongated, and have large vacuoles in the apical zone and nuclei in the basal zone. The antipodals of *I. sibirica* are of triangular shape.

The mature embryo sac, developing according to the Polygonum type, consists of a three-celled egg apparatus, typically three antipodal cells and two polar nuclei located near the center of the embryo sac. At the moment of pollination and fertilization the secondary nucleus occurs within the central cell in the embryo sac.

Fertilization, early stages of endosperm and embryo development. The pollen tube enters the embryo sac via the micropyle. Figure 5a shows the pollen tube inside the embryo sac where it destroys one synergid, leaving the other intact.

Synergids of *I. chrysographes*, *I. pseudacorus*, *I. setosa* and *I. sanguinea* become deformed after the pollen tube penetrates into the embryo sac. Synergids of *I. sibirica* persist until the formation of a multinucleate nuclear endosperm.

Figure 5e, f shows the three-celled egg apparatus after pollination. The pollen tube releases two sperm cells into the synergid cytoplasm.

One of the sperm cells then moves toward and fuse with the egg cell, which results in the formation of a zygote. Fertilized egg cell has two nucleoli, the smaller one presumably contributed by the male nucleus (Fig. 5e).

Another sperm cell fuses with the central cell to complete double fertilization and form the primary cell of the endosperm (Figs. 5c, 5d).

In *I. chrysographes* the process of sperm nuclear fusion and formation of the secondary nucleus was observed on the second day after pollinations.

The nuclear division of the primary cell of the endosperm precedes the division of the zygote. The endosperm is initially nuclear. The nuclei are located in cytoplasmic strands which cross the central vacuole. Nuclei have from one to three nucleoli. In *I. pseudacorus* the number of nuclei increases up to seven. The nuclei heteromorphism were observed throughout the periphery of endosperm coenocyte of *I. setosa* and *I. pseudacorus*.

After double fertilization the zygote passes a short period of rest. In *I. setosa* this period lasts about 7 days from the moment of fertilization.

During the first zygote division, the cell wall originates transversely. The two-celled embryo in *I. pseudacorus* ovules can be observed on the sixth day and in *I. setosa* on the ninth day after pollination (Fig. 5g). Then a longitudinal cell wall originates in the apical cell and a transverse cell partition originates in the basal cell. A four-cell embryo resembles a T-shaped structure (Fig. 5h).

Aberrant development of ovules and embryo sacs. Aberrant ovules were observed in all species studied. In *I. chrysographes* some ovules are small in size with lengths less than 260 μm. Also only one integument develops instead of two and the embryo sac fails to develop at all (Fig. 6a).

Such aberrant development occurs as a result of deviations in the initial formation of integuments.

In *I. sibirica* several cases of ovule degeneration were observed. These ovules are characterized by the abnormal growth of chalaza tissues and the absence of embryo sacs (Fig. 6h). In a single case the development of two ovules with a joint outer integument was noticed.

In *I. typhifolia* we observed the absence of embryo sacs in some completely formed ovules with developed nucellus (Fig. 6c). The nucellus is differentiated into a postament and a podium, and contains layers of pari-

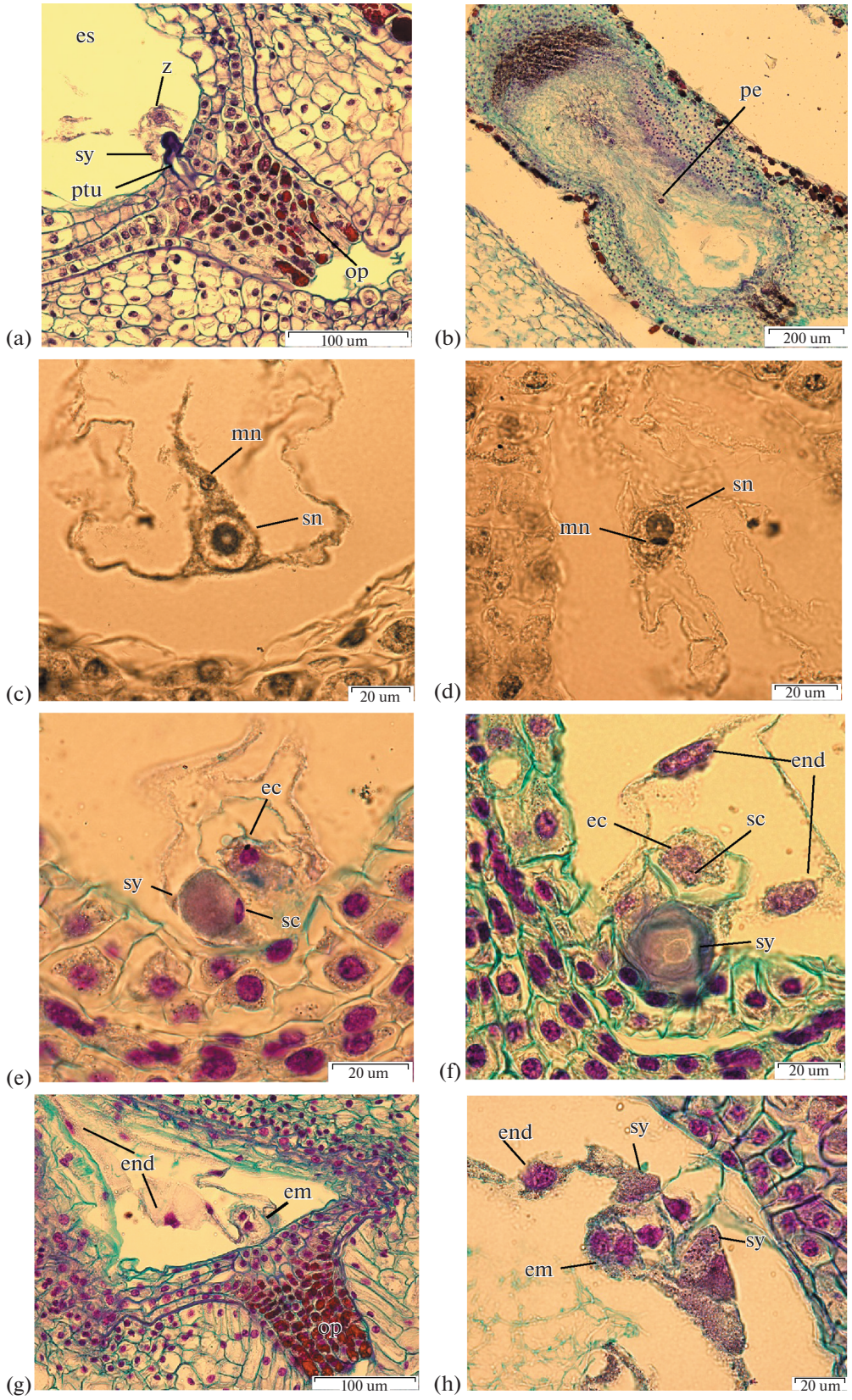

Fig. 5. Fertilization, early development stages of endosperm and embryo. a – *I. setosa*, zygote and pollen tube, ×400; b – *I. setosa*, primary endosperm nucleus, ×100; c, d – *I. sibirica*, secondary nucleus in the central cell and male nuclei, ×1500; e, f – *I. pseudacorus*, three-celled egg apparatus after pollination, ×1500; g – *I. setosa*, 2-cell stage embryo, ×400; h – *I. setosa*, 4-cell stage embryo, ×1500.

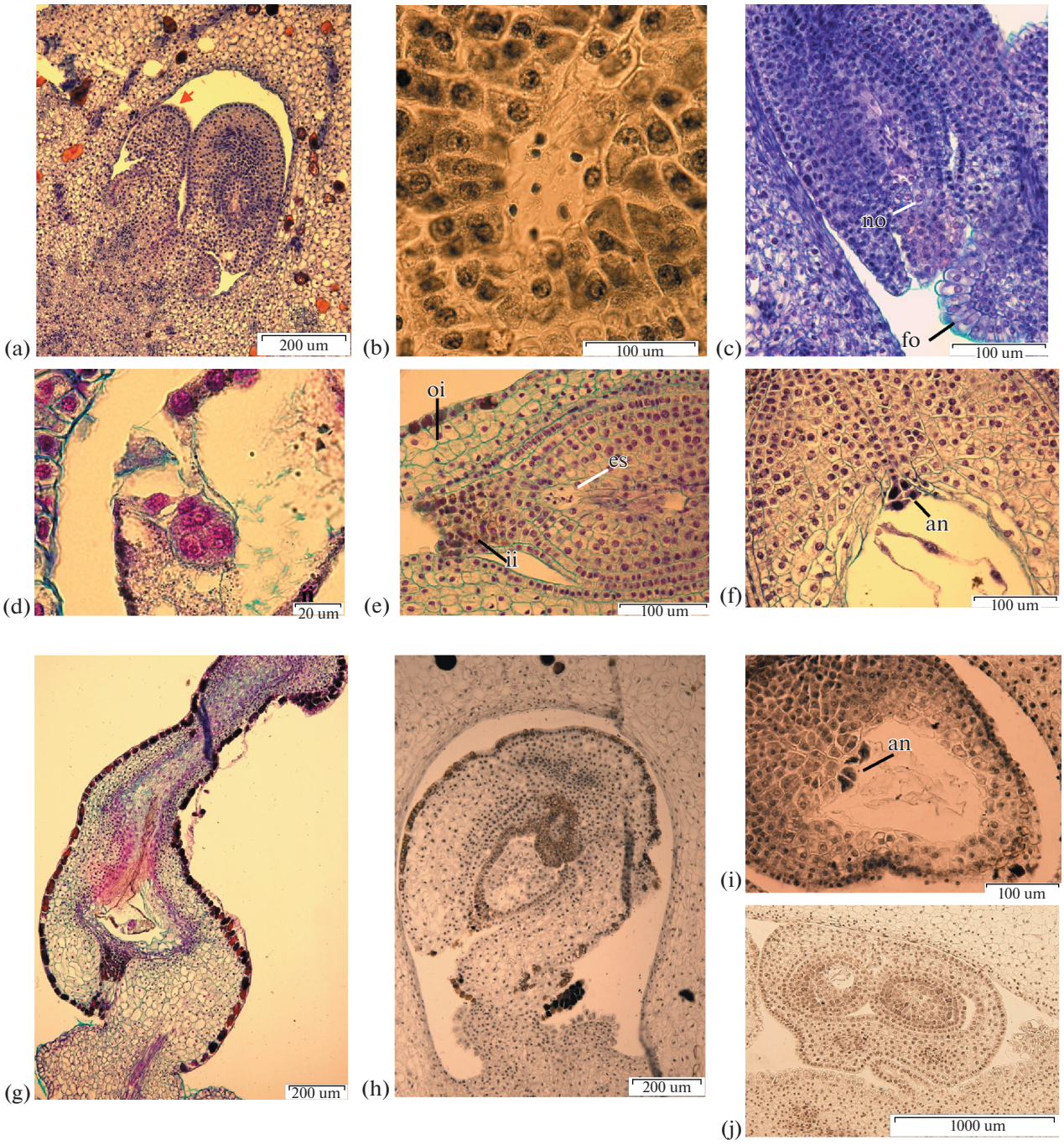

Fig. 6. Aberrant development of ovules and embryo sacs. a – *I. chrysographes* bud 35 mm, aberrant ovule, ×100; b – *I. sibirica*, undifferentiated nuclei in embryo sac, ×400; c – *I. typhifolia*, aberrant ovule, ×400; d – *I. setosa*, embryo, ×1500; e – *I. setosa* bud 60 mm, undifferentiated nuclei in embryo sac, ×400; f – *I. setosa*, antipodals, ×400; g – *I. setosa*, degenerate ovule, ×100; h – *I. sibirica*, aberrant ovule, ×400; i – *I. sibirica*, antipodals, ×400; g – *I. sibirica*, two ovules with a joint outer integument, ×40.

etal tissue. The tightly closed nucellus cells are located at the site of an embryo sac.

It was noticed that *I. sibirica*, *I. setosa* and *I. sanguinea* had completely formed ovules with aborted embryo sacs having undifferentiated nuclei (Figs. 6b, 6e).

A part of some *I. setosa* ovules degenerate, strongly deform and compress after fertilization. The nuclear division of primary cell of endosperm does not occur (Fig. 6g).

In *I. setosa*, in some cases embryo formation via free zygote divisions in the deformed ovules at the

stage of nuclear endosperm development is found (Fig. 6d). Such an embryo resembles in appearance the coenocytic prenatal formation of Paeoniaceae, first described by Yakovlev (1961).

DISCUSSION

In studied species the ovaries have axile placentation, the ovule is bitegmic, crassinucellate and anatropous, which was previously reported for other members of the genus *Iris*. The embryo sac is of the monosporic, eight-nucleate type. The Polygonum type of female gametophyte is the most common in angiosperms and is considered a primitive embryological character.

The present study includes several new observations for the genus. During megasporogenesis, a second meiotic division produces a T-shaped or linear tetrad of megaspores. The differences of microspore tetrad shape may be the result of random orientation of the cell plate during cell division. This is in agreement with the findings of Zhang (2011) working on *I. mandshurica* and Fan (2019) working on *I. sanguinea*. The megaspore tetrads of *I. sanguinea* are linear, T-shaped or juxtaposed. The megaspore tetrads of *I. mandshurica* are always linear. The megaspore on the chalaza becomes the functional spore.

In the micropyle region the cells are elongated radially and glandular in appearance. These cells represent an inner integumentary obturator of *I. sibirica*. The same radially elongated cells in the micropyle area where observed in *I. tenax* (Wilson, 2001). Previous studies have suggested that obturators are considered to assist in directing pollen tubes toward ovules and into the micropyle (Maheshwari, 1950). Wilson (2001) reports that it is likely that a similar function can also be attributed to the integumentary cells lining the micropyle.

In *I. sanguinea* and *I. typhifolia* nucellar epidermis cells are radially elongated in the micropyle area. These cells represent a nucellar obturator.

In *I. ensata*, *I. sibirica*, *I. pseudacorus*, *I. chrysographes* and *I. setosa* cells of the nucellar epidermis undergo periclinal divisions and form a nucellar cup.

The inner integument surrounding the nucellus is uniformly two cells in thickness and much thicker than the outer integument, which is 4–10 cells thick. In studied species the outer integument has a variable number of cell layers (Table 1).

The parietal cell divides both anticlinally and periclinally in these species. The development of parietal tissue also varies among the studied species. No more than 1–4 layers of parietal cells were observed (Table 1).

In the course of this study, a filiform apparatus was found in synergids of *I. sibirica* and *I. sanguinea*. The filiform apparatus consists of long wall ingrowths and is thought to function by directing the pollen tube into one of the synergids (Russell, 1992).

In *I. setosa*, *I. pseudacorus* and *I. typhifolia* the polar nuclei fusion occurs after the flower opens. Lee W. Lenz (1956) reports that in many cases, at the time of the opening of *I. munzii* flower, the polar nuclei have not yet approached and the fusion may be delayed as much as 72 hours after pollination. Wilson (2001) reports that development of a seven-celled megagametophyte occurs during the final floral bud stage in *I. tenax*. The fusion of the two polar nuclei to form a secondary nucleus must occur rapidly in *I. tenax* before the flower opens.

The previous studies on the development of ovules and embryo sacs of *Iris* species do not contain the description of such ovule characters as the length of the outer integument relative to the inner, and the presence of inner integumentary obturator, nucellar obturator and nucellar cap. In the study of Wilson (2001, Fig. 24) in the ovule of *I. tenax* it can be observed that cells of nucellar epidermis in the micropyle area become radially elongated and highly glandular in appearance. It can be assumed, that these cells represent a nucellar obturator. In the ovule of *I. tenax* the outer and inner integuments are of equal length (Wilson, 2001, Figs. 19, 24, 29, 31).

In the three species of the *Sibiricae* series (*I. sanguinea*, *I. typhifolia*, *I. sibirica*), the presence of additional obturators in the ovules other than the funicular obturator was revealed (Fig. 7). Areas with radially elongated, vacuolated cells in the micropyle pole where identified. *I. sanguinea* and *I. typhifolia* have nucellar obturator whereas *I. sibirica* has integumentary obturator.

In *I. sanguinea*, *I. typhifolia* and *I. chrysographes*, from series *Sibiricae*, the outer and inner integuments are of equal length (Figs. 2a, 2d, 2g). In *I. pseudacorus*, *I. ensata* and *I. sibirica*, from series *Laevigatae*, the outer integument is at least 48 ± 2 μm shorter than the inner (Figs. 2b, 2c, 2e). The outer integument of *I. setosa* from series *Tripetalae* is also at least 68 ± 16 μm longer than the inner (Fig. 2f).

The study describes the most significant characters of the ovule and embryo sac, such as nucellar cap, funicular obturator, inner integumentary obturator and filiform apparatus into the sinergids. Obtained data can be also used for future studies of the reproductive system in Iridaceae.

Appendix 1. List of taxa with GenBank-EMBL accession numbers used in the analyses

The numbers are written in the order of loci: *matK*, *trnL with trnL-F IGS*, *ycf1*

Table 1. Ovule and embryo sac structure and development

Species	Mature embryo sac (length × width. μm; length to width ratio)	Parietal tissue	Nucellar epidermis	Inner integument	Outer integument	Vascular bundle	Antipodals	Synergids	Endosperm
1	*2*	*3*	*4*	*5*	*6*	*7*	*8*	*9*	*10*
series *Laevigatae* I									
I. pseudacorus	633 ± 12 × 382 ± 9 1.7:1	–	nucellar cap, 2 layers	2 layers, at the micropyle area expands to form up to 3–5 layers, form operculum	5–7 layers, shorter than the inner integument	reaches the chalaza	3, persist until four-celled embryo formation	deformed after the pollen tube penetrates into the embryo sac	nuclear, heteromorphism of nuclei
series *Laevigatae* II									
I. ensata	501 ± 8 × 380 ± 6 1.3:1	1–2 layers	nucellar cap, 2 layers	2 layers, at the micropyle area expands to form up to 4–5 layers, form operculum	7–8 layers, shorter than the inner integument	reaches the chalaza	3	–	nuclear
series *Tripetalae*									
I. setosa	820 ± 55 × 462 ± 46 1.8:1	2 layers	nucellar cap, 2–3 layers	2 layers, at the micropyle area expands to form up to 6 layers, form operculum	5–6 layers, expands to 7–10 layers in the micropyle area, tapers to the edge, longer than the inner integument	reaches the chalaza	3–4, persist until four-celled embryo formation	deformed after the pollen tube penetrates into the embryo sac	nuclear, heteromorphism of nuclei
series *Sibiricae*									
I. chrysographes	420 ± 24 × 299 ± 28 1.4:1	1–2 layers	nucellar cap 2 layers	2 layers, at the micropyle area expands to form up to 3 layers, form operculum	8–9 layers, outer and inner integuments are of equal length	extends through the chalaza to the middle of the outer integument	3, persist until nuclear endosperm formation	deformed after the pollen tube penetrates into the embryo sac	nuclear
I. sanguinea	1606 ± 32 × 901 ± 24 1.8:1	2–4 layers	nucellar obturator	2 layers, at the micropyle area expands to form up to 3–5 layers, form operculum	5 layers, outer and inner integuments are of equal length	reaches the chalaza	3, deformed at the beginning of the development endosperm	deformed after the pollen tube penetrates into the embryo sac	nuclear
I. typhifolia	919 ± 39 × 464 ± 48 2:1	2 layers	nucellar obturator	2 layers, at the micropyle area expands to form up to 4 layers, form operculum	8–9 layers, outer and inner integuments are of equal length	reaches the chalaza	3	–	nuclear
I. sibirica	1136 ± 36 × 681 ± 27 1.7:1	2 layers	nucellar cap, 2 layers	2 layers, at the micropyle area expands to form up to 3 layers, form integumentary obturator	4–6 layers, shorter than the inner integument	reaches the chalaza	3–4, deformed at the beginning of the development endosperm	persist until the formation of a multinuclear nuclear endosperm	nuclear

Note: Dash (–) – not observed in this material.

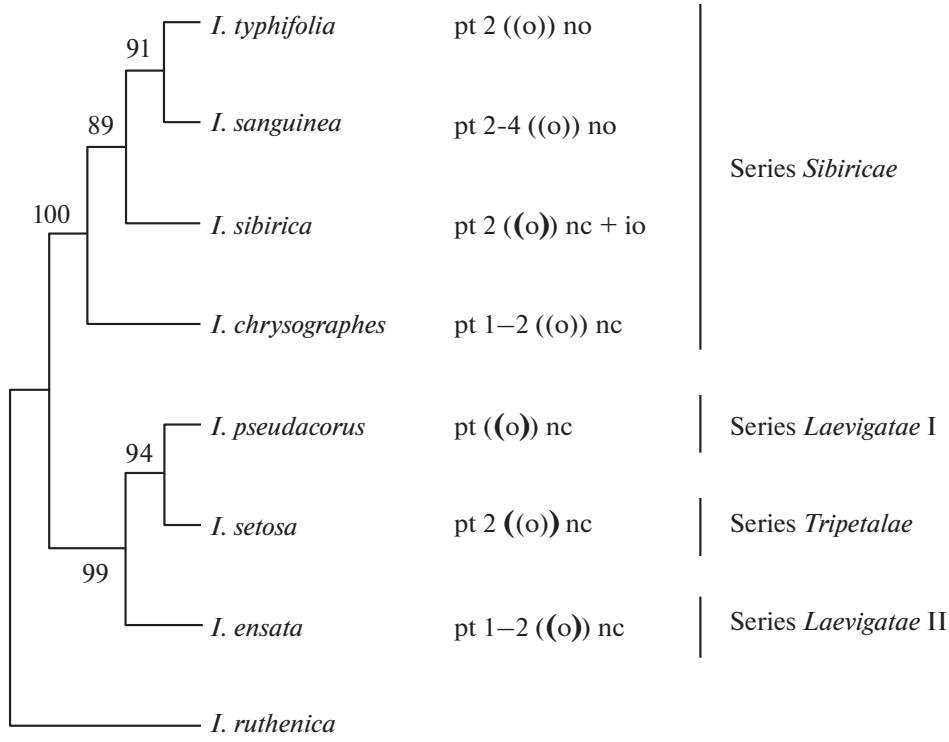

Fig. 7. Maximum likelihood tree resolved using *matK*, *trnL*, *trnL-F IGS*, *ycf1* sequence data for 8 species in *Iris* subgenus *Limniris*. *I. ruthenica* established as an outgroup. Bootstrap percentage values are given above branches. Series names are given according the classification by Mathew (1989). pt – parietal tissue, nc – nucellar cap, no – nucellar obturator; io – inner integumentary obturator. ((o)) – the outer integument is shorter than the inner; ((o)) – the outer integument is longer than the inner; ((o)) – the outer and inner integuments are of equal length.

Iris chrysographes FJ197270 LR597379 KP089512; *I. ensata* FJ197276 LT628002 KP089520; *I. pseudacorus* KC118959 LT628004 KP089531; *I. ruthenica* FJ197296 EU939495 KP089534; *I. sanguinea* LC373218 EU939496 KP089535; *I. setosa* KC118938 EU939498 KP089538; *I. sibirica* KX676790 LT984482 KP089539; *I. typhifolia* KC118942 EU939514 KP089547

ACKNOWLEDGMENTS

The investigation was partially supported by the Comprehensive Program of an Institutional Research Project "Vascular plants of Eurasia: taxonomy, flora, plant resources" (No. AAAA-A19-119031290052-1) of the Komarov Botanical Institute of the Russian Academy of Sciences. The authors are grateful to the scientist of the Perm State University, Department of Botany and Genetics of Plants, Dr. Valentina Vereshchagina for help and consultations, and to the curator of the collection of Irises in Iridarium of the Peter the Great Botanical Garden, Dr. Nina Alexeeva for provision of plant materials.

REFERENCES

Alexeeva N. 2005. Species of *Iris* genus in Russia. The problems of preservation in situ and introduction. Ph.D. thesis. Komarov Botanical Institute of Russian Academy of Sciences. 18 p. (In Russ.).

Alexeeva N. 2006. Generis *Iris* L. (Iridaceae) species nova e Republica Altai. – Novitates systematicae plantarum vascularium. 38: 116–119 (In Russ.).

Alexeeva N. 2008. Genus *Iris* L. (Iridaceae) in the Russia. – Turczaninowia. 11 (2): 5–68 (In Russ.).

Alexeeva N. 2013. *Iris lokiae*, a new species of genus *Iris* (Iridaceae). – Botanicheskii Zhurnal. 98 (11): 1415–1420 (In Russ.).

Alexeeva N. 2018. New species of *Iris* L. (Iridaceae) from Mongolia. – Turczaninowia. 21 (4): 145–149 (In Russ.).
https://doi.org/10.14258/turczaninowia.21.4.14

Barykina R.P., Veselova T.D., Devyatov A.G., Dzhalilova Kh.Kh., Ilina G.M., Chubatova N.V. 2004. Handbook of Botanical microtechnology. Basics and methods. MSU, Moscow, 312 p. (In Russ.).

Boltenkov E., Artyukova E., Kozyrenko M., Trias-Blasi A. 2018. *Iris tibetica*, a new combination in I. ser. *Lacteae* (Iridaceae) from China: evidence from morphological and chloroplast DNA analyses. – Phytotaxa, 338 (3), 223–240.
https://doi.org/10.11646/phytotaxa.338.3.1

Dong W., Xu C., Li C., et al. 2015. *ycf*1, the most promising plastid DNA barcode of land plants. *Sci Rep*. 5: 8348. Published 2015 Feb 12.
https://doi.org/10.1038/srep08348

Dong X.D., Zhao H., Zhao Y.T. 1997. A New Species of *Iris* from Yunnan. – Acta Phytotaxon. Sin. 35 (1): 81–82.

Dykes W.R. 1913. The genus *Iris*. Cambridge. 245 p.

Edgar R.C. 2004. MUSCLE: multiple sequence alignment with high accuracy and high throughput. – Nucleic Acids Res., 32 (5): 1792–1797. https://doi.org/10.1093/nar/gkh340

Fan L., Hasenstein K.H., Wang L. 2019. Embryology of *Iris sanguinea* Donn ex Horn. and its systematic relationship. – J. Forestry Res. 1–14. https://doi.org/10.1007/s11676-019-01039-z

Fenneman E., Graham S. 2016. DNA Barcoding the Vascular Plant Flora of Southern British Columbia. Figshare. https://doi.org/10.6084/m9.figshare.4012332.v1

Güner A., Duman H. 2007. A New Juno Iris from Northeast Anatolia, Turkey. – Turk. J. Bot. 31: 311–315.

Guo J., Wilson C.A. 2013. Molecular phylogenetic study of the crested *Iris* based on five plastid markers. – Syst. Bot. 38 (4): 987–995. https://doi.org/10.1600/036364413X674724

Haeckel I. 1930. Über Iridaceen. – Flora oder Allgemeine Botanische Zeitung. 125 (1): 1–82. https://doi.org/10.1016/S0367-1615(17)31778-0

Kamelina O.P., Proskurina O.B., Zhinkina N.A. 1992. On the method of staining of xembryological preparations. – Bot. Zhurn. 77 (4): 93–96 (In Russ.).

Karagyozova M. 1963. Embryological studies on *Iris pseudacorus* L. – Bulgarische Akademie der Wissenschaften. 11: 111–124.

Kumar S., Stecher G., Li M., Knyaz C., Tamura K. 2018. MEGA X: Molecular Evolutionary Genetics Analysis across computing platforms. – Mol. Biol. Evol. 35: 1547–1549.

Lawrence G.H.M. 1953. A reclassification of the genus *Iris*. – Gentes Herbarum. 8 (4): 346–371.

Lenz L.W. 1956. Development of the Embryo Sac, Endosperm and Embryo in *Iris Munzii* and the Hybrid *I. Munzii* x *I. sibirica* 'Caesar's Brother'. – Aliso. 3 (3): 329–343. https://doi.org/10.5642/aliso.19560303.06

Li N., Dong Y.Z., Liang F.L. 2005. Studies on microsporogenesis and the formation of malegametophyte in *Iris blowdowill*. – Bull. Bot. Res. 25: 140–143.

Mathew B. 1989. The *Iris*. London: Batsford Ltd. 202 p.

Mavrodiev E.V., Martínez-Azorín M., Dranishnikov P., Crespo M.B. 2014. At least 23 genera instead of one: the case of *Iris* L. s.l. (Iridaceae). – PLoS One. 9 (8): e106459. https://doi.org/10.1371/journal.pone.0106459

Mermygkas D., Kit T., Yannitsaros A. 2010. A new species of *Iris* (Iridaceae) from the northern Peloponnese (Greece). – Phytologia Balcanica. 16 (2): 263–266.

Mitic B. 2002. *Iris adriatica* (Iridaceae), a New Species from Dalmatia (Croatia). – Phyton (Horn, Austria). 42 (2): 305–314.

Mizuno T., Okuyama Y., Iwashina T. 2018. Flavonoids from *Iris sanguinea* var. *tobataensis* and chemotaxonomic and molecular phylogenetic comparisons with *Iris sanguinea* var. *sanguinea*. Bulletin of the National Museum of Nature and Science, Series B. 44: 135–145.

Pande P.C., Singh V. 1981. A contribution to the embryology of the *Iridaceae*. – J. Ind. Bot. Soc. 60: 160–167.

Pausheva Z.P. 1988. Plant Cytology Practical Training. Moscow. 271 p. (In Russ.).

Pearse A.G.E. 1962. Histochemistry, theoretical and applied. Moscow. 961 p. (In Russ.).

Poddubnaya-Arnoldi V.A. 1976. Cytoembryology of angiosperms, principles and perspectives. Nauka, Moscow. 507 p. (In Russ.).

Riley H.P. 1942. Development of the embryo sac of *Iris fulva* and *I. hexagona* var. *giganticaerulea*. – Transactions of the American Microscopy Soc. 61 (4): 328–335. https://doi.org/10.2307/3222898

Rodionenko G.I. 1961. The genus *Iris* L. (Voprosi morfologii, biologii, evolutsii i sistematiki). Academia Nauk SSSR, Moscow-Leningrad, 216 p. (In Russ.).

Rodionenko G.I. 2007. On the independence of genus *Limniris* (Iridaceae). – Botanicheskii Zhurnal (St Petersburg). 92: 547–554 (In Russ.).

Rudall P.J., Owens S.J., Kenton A.Y. 1984. Embryology and breeding systems in Crocus (Iridaceae) – a study in causes of chromosome variation. – Plant Syst. Evol. 148 (1–2): 119–134. https://doi.org/10.1007/BF00984573

Shamrov I.I. 2008. Ovule of flowering plants: structure, functions, origin. Moscow: KMK Scientific Press Ltd. 350 p. (In Russ.).

Smith F.H., Clarkson Q.D. 1956. Cytological studies of interspecific hybridization in *Iris*, subsection *Californicae*. – Am. J. Bot. 43: 582–588. https://doi.org/10.1002/j.1537-2197.1956.tb10538.x

Sokolov I.D. 1983. The study of endosperm cells filling the central part of tile embryo sac (nuclear type of the endosperm). – Botanicheskii Zhurnal (St Petersburg). 58 (10): 1333–1341 (In Russ.).

Sokolov I.D., Petrov A.P., Kramarenko Yu.P. 1974. Dynamics of cell formation in the endosperm of *I. pseudacorus* L. and *I. pumila* L. – Botanicheskii Zhurnal (St Petersburg). 1974. 59 (11): 1576–1582 (In Russ.).

Wheeler A.S., Wilson C.A. 2014. Exploring Phylogenetic Relationships within a Broadly Distributed Northern Hemisphere Group of Semi-Aquatic *Iris* Species (Iridaceae). – Syst. Bot. 39 (3), 759–766. https://doi.org/10.1600/036364414X681482

Sokolovskaya T.B., Shpilevoj B.E. 1990. The family Iridaceae. In: Yakovlev M.C., editor. Comparative embryology of flowering plants. V. 5. Butomaceae – Lemnaceae. Leningrad: Nauka. P. 129–134 (In Russ.).

Tamura K., Nei M. 1993. Estimation of the number of nucleotide substitutions in the control region of mito-

chondrial DNA in humans and chimpanzees. – Mol. Biol. Evol. 10: 512–526.

Tillie N., Chase M.W., Hall T. 2001. Molecular studies in the genus *Iris* L.: a preliminary study. – Int. conference of *Irises* and *Iridaceae*: Biodiversity and Systematics, Rome, Italy. Ann. Bot. Nuova Serie. 1 (2): 105–112.

Yasui K., Sawada N. 1940. On the spore and embryo sac formation with special reference to the sterility of *Iris japonica* Thunb. – Botanical Magazine, Tokyo. 54 (639): 96–102. https://doi.org/10.15281/jplantres1887.54.96

Wilson C.A. 2001. Floral stages, ovule development, and ovule and fruit success in *Iris tenax*, focusing on var. *gormanii*, a taxon with low seed set. – Am. J. Bot. 88 (12): 2221–2231. https://doi.org/10.2307/3558384

Wilson C.A. 2004. Phylogeny of Iris based on chloroplast matK gene and trnK intron sequence data. – Mol. Phylogen. Evol. 33 (2): 402–412. https://doi.org/10.1016/j.ympev.2004.06.013

Wilson C.A. 2006. Patterns of evolution in characters that define *Iris* subgenera and sections. – Aliso. 22: 425–433.

Wilson C.A. 2009. Phylogenetic relationships among the recognized series in *Iris* section *Limniris*. – Syst. Bot. 34 (2): 277–284. https://doi.org/10.1600/036364409788606316

Wilson C.A. 2011. Subgeneric classification in *Iris* re-examined using chloroplast sequence data. – Taxon. 60 (1): 27–35. https://doi.org/10.1002/tax.601004

Zhang D., Wang L., Zhuo L.H. 2011. Embryology of *Iris mandshurica* Maxim. (Iridaceae). – Plant Syst. Evol. 293 (1/4): 43–52. https://doi.org/10.1007/s00606-011-0427-1

Zhao Y.T. 1992. A New Species of *Iris* from China. – Acta Phytotaxon. Sin. 30 (2): 181–182.

СРАВНИТЕЛЬНОЕ ИССЛЕДОВАНИЕ СТРОЕНИЯ И РАЗВИТИЯ СЕМЯЗАЧАТКОВ НЕКОТОРЫХ ВИДОВ *IRIS* ПОДРОДА *LIMNIRIS* (IRIDACEAE)

М. М. Дорофеева[a,b,#], П. М. Журбенко[a,##]

[a] *Ботанический институт им. В.Л. Комарова РАН ул. Проф. Попова, 2, Санкт-Петербург, 197376, Россия*

[b] *Санкт-Петербургский государственный лесотехнический университет имени С.М. Кирова Институтский пер., 5, Санкт-Петербург, 194021, Россия*

[#] *e-mail: drofa88@mail.ru*

[##] *e-mail.: pj_28@mail.ru*

Описаны наиболее значимые эмбриологические признаки строения семязачатков и зародышевых мешков, такие как нуцеллярный колпачок, фуникулярный обтуратор, интегументальный обтуратор, нуцеллярный колпачок и нитчатый аппарат в синергидах, у 7 видов рода *Iris*, относящихся к подроду *Limniris*: *Iris chrysographes*, *I. ensata*, *I. pseudacorus*, *I. sanguinea*, *I. setosa*, *I. sibirica*, *I. typhifolia*. Показано, что эти признаки вариабельны и могут быть использованы для уточнения систематики рода.

Ключевые слова: род *Iris*, *Limniris*, систематика, семязачаток, зародышевый мешок, обтуратор, нуцеллярный колпачок

БЛАГОДАРНОСТИ

Исследование частично проведено в рамках выполнения государственного задания согласно тематическому плану Ботанического института имени В.Л. Комарова РАН по теме “Сосудистые растения Евразии: систематика, флора, растительные ресурсы” (регистрационный № АААА-А19-119031290052-1). Авторы выражают особую благодарность сотруднику кафедры ботаники и генетики растений Пермского государственного университета, профессору В.А. Верещагиной за помощь и консультации, а также куратору коллекции касатиковых на Иридарии Ботанического сада Петра Великого, ст. науч. сотр. Н.Б. Алексеевой за предоставление растительных материалов.